

X-57 Traction Power and Command Systems Development

Sean Clarke¹, Jacob Terry¹, Keith Harris² & David Avanesian³

¹NASA Armstrong Flight Research Center, Edwards, California, 93523, USA
 ²NASA Langley Research Center (Retired), Hampton, Virginia, 23681, USA
 ³NASA Glenn Research Center, Cleveland, Ohio, 44135, USA

Abstract

This paper describes the final, as-built design of the X-57 Maxwell aircraft power and command system architecture that implements the electrified propulsion capability. The development of the traction power, command, and avionics power subsystems proceeded as planned at the initial project critical design review, but improvements to the design were identified following the development of detailed operations concepts and integrated subsystem and system testing. The redundant architecture with A-side and B-side buses provided a robust framework for a developmental system that would turn out to have a lower technology readiness than had been assumed upon project formulation. As the project team identified reliability or performance gaps in the electrified propulsion powertrain components and their interactions with the other vehicle systems, the traction power, command, and avionics architectures were modified to accommodate the modified systems.

Following the publication of the planned design approach at the critical design review milestone [1], the project team developed the flight hardware and software, integrated the systems, and adjusted the design and qualification activities to address gaps in the components, system architecture, and requirements as the gaps were realized. In addition to inherent challenges in development of these subsystems, the integration of this new technology with adjacent critical systems in an aircraft configuration posed additional challenges that drove design considerations across the subsystem development and the other vehicle systems. Integration complications included electromagnetic compatibility, thermal performance, and tolerance of single-point failures internal and external to the powerplant. Development of a qualification program was required for the new motors, inverters, and batteries, and hardware performance during component qualification fed back into the development process and led lessons learned and redesign of key elements.

Keywords: distributed propulsion, electric propulsion, electrified powertrains, system design, redundancy

1 Introduction

The X-57 Maxwell is an experimental aircraft that showcases an aerodynamic design optimized for high-speed cruise with a high-aspect ratio wing and propellers integrated in the wingtips and distributed along the leading edge to provide high-lift performance for low-speed maneuvers including take-off and landing. The integration of this distributed propulsion system relies on an electrified propulsion system using lithium-ion batteries in the aircraft cabin for energy storage and high-efficiency, air-cooled siliconcarbide metal oxide field effect transistor (SiC MOSFET) inverters and direct-drive motors embedded in distributed nacelles along the wing for conversion of the electrical power to propeller shaft torque. To highlight the essential technology of the electric powertrain, the aircraft was designated *Maxwell* in reference to James Clerk Maxwell's foundational work describing the electromagnetic forces that enable the motors, inverters, and batteries in the X-57 traction system.

The combination of the aerodynamic design for increased efficiency at high-speed cruise and the integration of the advanced electric powertrain results in an improvement of cruise efficiency of 4.8x while maintaining the low-speed performance of the baseline vehicle [2]. While the X-57 project concluded before the aircraft systems were demonstrated in flight test, the development, integration, and ground test activities provided key insights into the challenges associated with the new electrified technologies.

The development approach of the project was to base the design of the X-57 Maxwell on the Tecnam P2006T (Costruzioni Aeronautiche Tecnam S.r.l., Capua, Italy) airframe and modify that design with a retrofitted high aspect-ratio wing and an electrified powertrain. A new wing was designed [3], fabricated with considerations for power and flight control system integration [4], and qualified for the full flight envelope [5]. The powerplant systems including the internal combustion engines, fuel storage and distribution, and associated cockpit instruments were replaced with electric motors and inverters and a lithium-ion battery system. In addition to the electric motors used for primary propulsion, the new wing was designed to employ an array of smaller electric motors and propellers distributed across the leading edge of the wing, which would provide high-lift during low-speed flight.

The benefits of propulsion airframe integration (PAI) techniques demonstrated in the X-57 configuration are made possible by the advent of electric propulsion components that promise lightweight, reliable performance with exceptional efficiency. This offers aircraft designers a range of new options for vehicle architectures, including the distributed propulsion capability demonstrated here and electric vertical take-off and landing (eVTOL) vehicles that may provide new urban mobility opportunities. Motor and controllers offer improved scaling characteristics that allow aircraft designers to consider multiple small propulsors installed in aircraft locations while maintaining the system performance of a large, centralized propulsor unlike thermal conversion systems like turbine and piston engines which suffer from lower specific power at smaller scales. High-efficiency electric powertrains like the X-57 powerplant enable practical PAI designs, and the resulting aircraft with lower operating costs (via reduced energy and maintenance) offer increased accessibility for public use.

2 System Design Overview

The Traction Power and Command Systems were architected to support multiple aircraft configurations over the X-57 project life cycle. The initial driving configurations for the design of these subsystems were Mods II and III with an electrified powertrain integrated in the original wing for Mod III and in the retrofit wing for Mod III. The Mod IV configuration expands the requirements on these subsystems with the addition of the High Lift System, which had twelve additional motors requiring power and control from these subsystems.

The traction system development for Mod II and III (Figure 1) was completed largely as planned and initially published. The redundant architecture with an "A-side" and a "B-side" battery bank feeding A and B distribution buses and A and B inverters worked well. The 2,560 battery cells in each pack were divided into 8 modules instead of 4, and once the concept of operations had matured, it became clear that an external power disconnect for the ground crew or first responders was necessary.

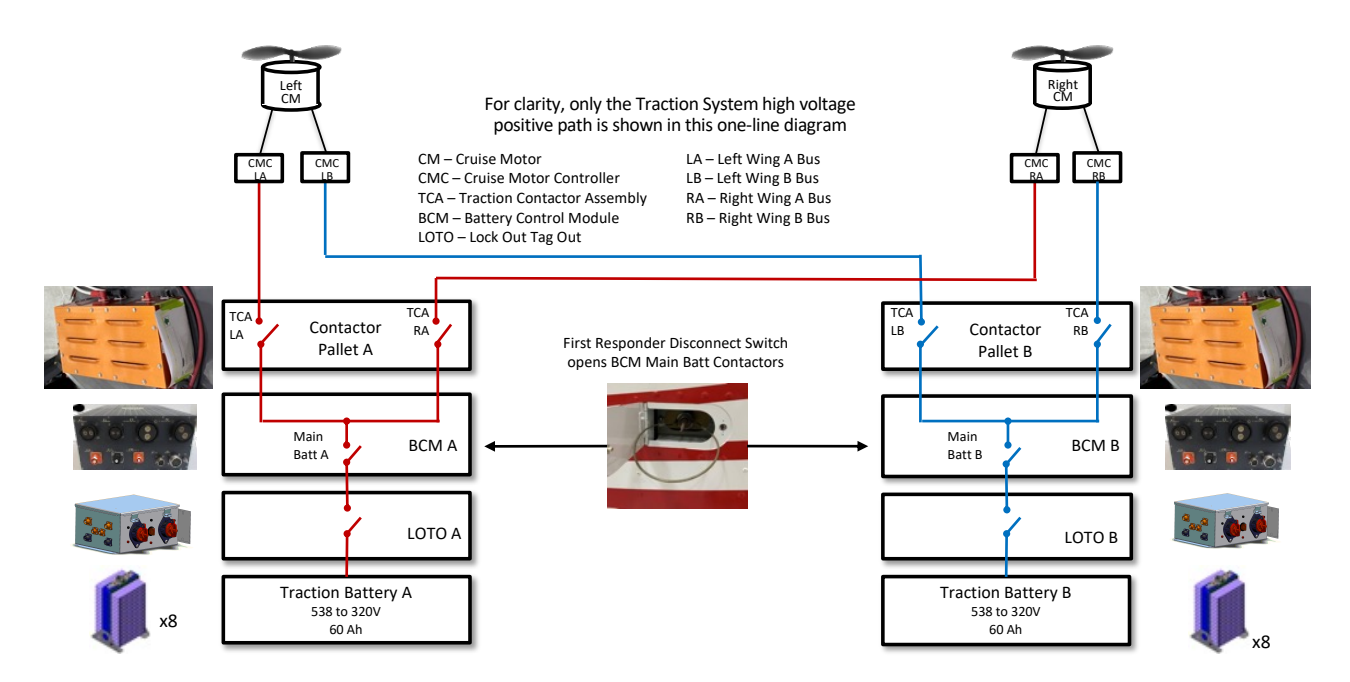


Figure 1 - Traction Power System, Mod II and III

The impacts of the Mod IV power and energy requirements were not known until detailed mission planning and performance testing of the components could be completed. The planned approach to add additional power distribution buses from the same battery packs to the new high-lift nacelles worked as expected with minor impacts to the required rating of the protection devices (Figure 2).

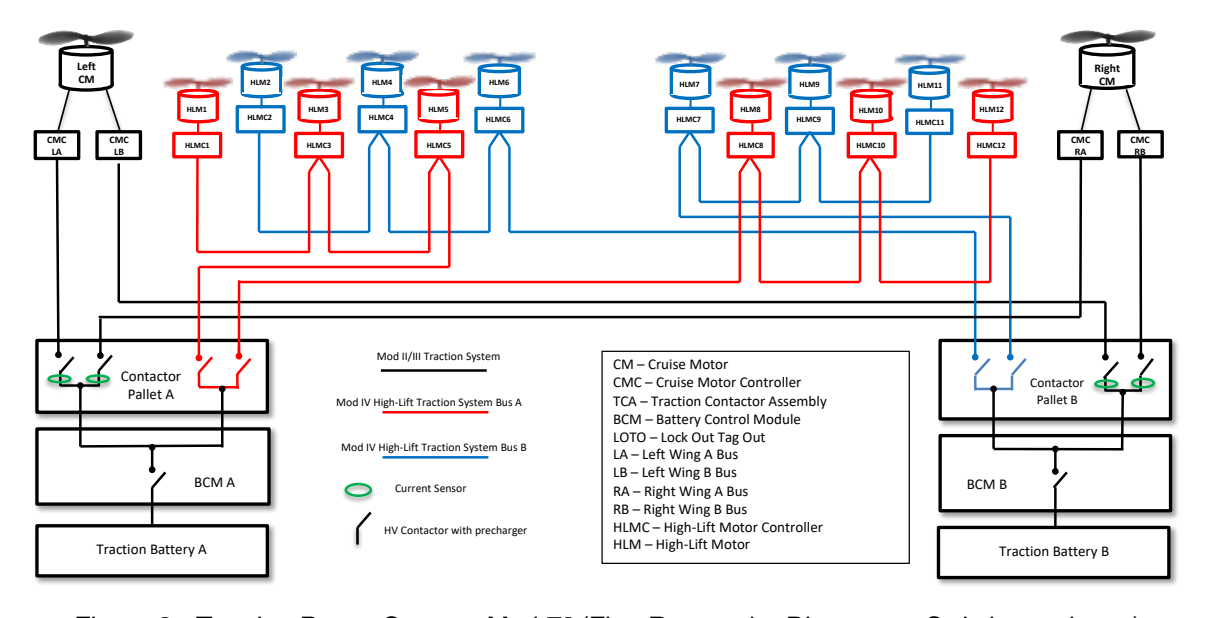


Figure 2 - Traction Power System, Mod ${
m IV}$ (First Responder Disconnect Switch not shown)

The command system architecture was also developed as planned with minor modifications over the course of the system integration and testing (see Figure 3). The "Controller Area Network (CAN) Relay" originally included in the design was deemed unnecessary, which simplified the system analysis as discussed below. Ports were added for ground support equipment interfaces that accommodated external bus logging and test message injection. The throttle lever encoders did not automatically boot into an operating state as originally designed, so additional command messages were required which had additional side effects which is discussed in Section 4.

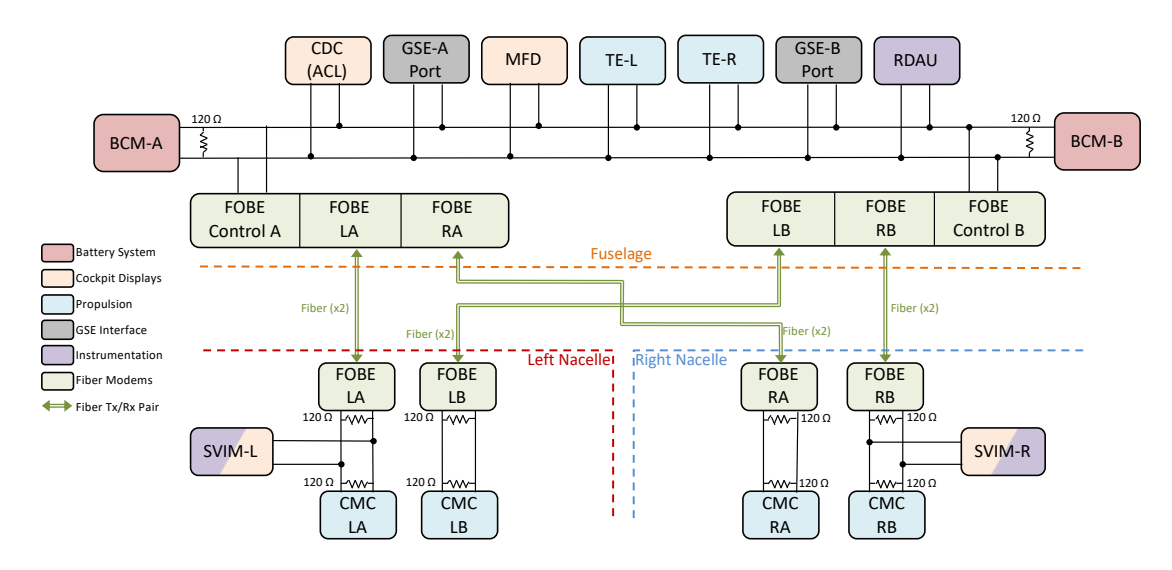


Figure 3 - Command System, Mod ${\rm II}$ and ${\rm III}$

The expansion of the command system for Mod IV did not extend the CAN Bus as planned at the critical design review and previously published, as the "Fiber Optic Bus Extender" (FOBE) modems would have required redesign to fit in the high-lift nacelles (see Figure 4). Instead, an Ethernet network was designed, and the High Lift Motor Controllers included an onboard fiber-optic Ethernet interface. The Mod IV systems enabled a novel automatic lift-augmentation capability and a higher performance take-off method that performed well in simulation [6].

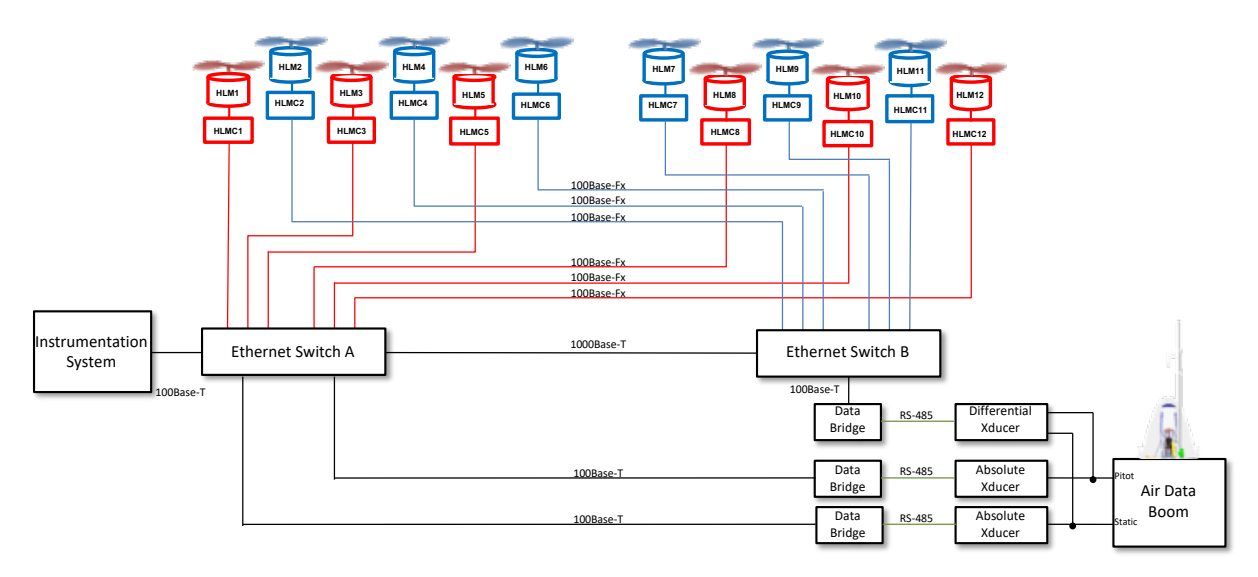


Figure 4 - Command and Data Handling network added to the Command System in Mod IV

The avionics power architecture development plan originally presented required much more detailed analysis for all possible failure modes and the energy and power requirements in each of those cases (Figure 5). As the aircraft systems were developed and detailed performance measurements could replace assumed loads, some branches were moved between buses. The wing avionics buses were converted to 23 V instead of the 13.8 V bus originally planned to provide additional margin above the minimum operating voltage of 9 V for the CMCs, FOBEs, and SVIMs. The feed power for the wing avionics buses was changed to the Essential Bus so that the aircraft could maintain propulsion if the 480 V/13.8 V DC/DC converters failed and the DC converter buses (similar to the "generator buses" in the original vehicle architecture) had to be shed.

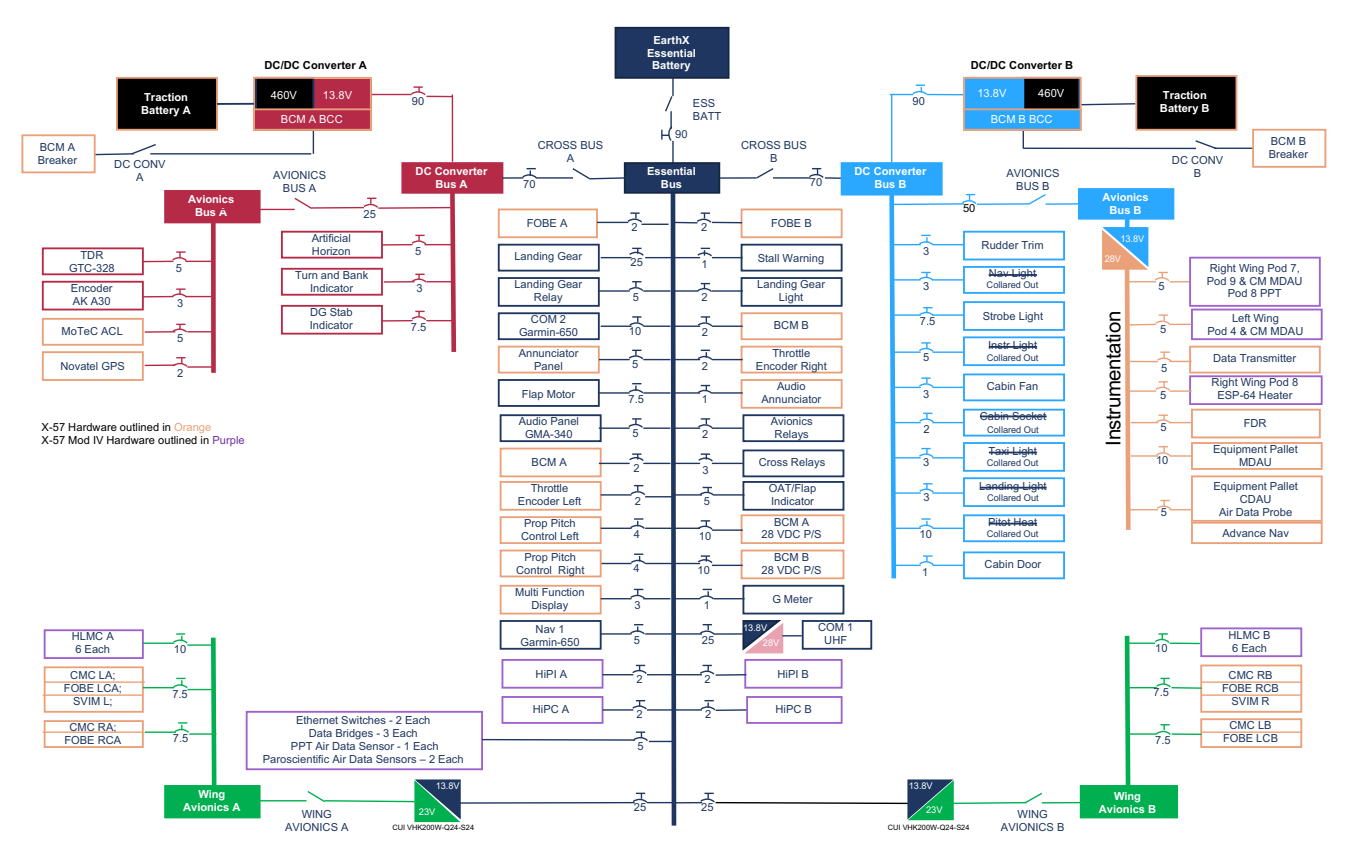


Figure 5 - Avionics Power Architecture (including Mod IV additions)

Overall, the system architecture laid out at the critical design review was successful. The redundancy approach of allocating half the energy storage, power distribution, and power conversion into isolated "A" and "B" sides provided the expected value in limiting hazard scope resulting from component failures. While this does not improve the hazard impact for common mode failures (e.g., design or technology defects), this was still valuable. The architecture also limited the types of failures that were credible by minimizing the number of interfaces between components that could fail. A more complex energy storage, power distribution, or power conversion architecture would allow the system to maintain closer to full power in various failure modes, but the increased complexity greatly increases the development overhead and could result in additional power conversion losses during nominal operation. Further details on the cockpit systems and the pilot workflow in the Mod configuration are available in [7].

3 Traction Power System

The traction power system development for the Mod II and III configuration (see Figure 1 and Figure 2) was successful and kept the overall architecture presented at the X-57 critical design review [1]. As there was not a separate hardware-in-the-loop development lab and system integration and testing required access to the aircraft, the "A/B" redundancy architecture was especially useful. The integration team was able to tailor test and operational procedures to select either facility ground support power or battery power depending on the test objective, and to limit power distribution to the specific inverter(s) that were installed on the aircraft or used for an individual test card. This was an effective high voltage hazard control feature. However, this capability required the individual bus power distribution control provided by the Contactor Pallets, adding weight and complexity to the power distribution buses. The advent of the contactor pallets was driven by the need for the pilot to be able to enable traction power individually for each motor controller (and to remove high voltage from a faulted motor inverter), providing more granular control than the Battery Control Module contactors. However, the contactors

in the Battery Control Module (BCM) were sized to interrupt traction power at high current and were therefore available for emergency action by the pilot. This flexibility with multiple contactors (A/B, L/R) in multiple locations (Battery Control Modules and Contactor Pallets) of the power distribution bus resulted in flexibility for the system prototyping, integration, and testing configurations. The development activities were often conducted on the airframe itself as a separate "iron bird" development bench was not constructed for the aircraft integration, so the ground support equipment was frequently configured for battery simulation mode with the aircraft traction system powered externally, and once the battery system was ready for integration, the ground support equipment was used for both battery charging and battery discharge testing procedures.

While the traction bus interfaces at the battery control modules and contactor pallets made reconfiguration over the course of development more practical, in some cases, there were minor hazards introduced. For example, in a troubleshooting or developmental configuration where a contactor pallet might be removed for repair, the system could not be used safely to test an inverter or motor because the dual output connectors of the battery control module were engaged by the same contactors meaning that the unused channel would have high voltage present without proper termination. This is primarily a challenge during the development phase of the project and would not have been an impact during flight operations once all the traction components had completed the acceptance test program and proven reliable.

The X-57 program drafted and maintained hazard description documents throughout the lifecycle of the project. These documents include all credible initial causes, their potential impact, mitigations that would be implemented to prevent the initiation of the event, and ameliorations that would reduce the impact if the hazardous condition was instantiated. As a result of the redundant architecture with components sized for single-string flight, many failures in the experimental components such as the battery modules, traction contactors, and inverters could be effectively mitigated by a pilot action to isolate the failed component and return to base under partial power. This had the side effect that the partial power case is a key configuration for many of the system analyses, but for a test program with a dedicated flight test arena, this was manageable for this test approach.

The power used at various operating conditions was a driving metric motivating the X-57 project activity. Propeller shaft power would have been a useful measurement, and while rotational speed was redundantly measured by the sensorless controller in the inverters and by an independent sensor, direct measurement of shaft torque was not proven accurate or reliable in the high electromagnetic interference environment around the motor (although torque sensors would have been evaluated in flight). The input power to the motor is a dual three-phase electrical interface with high frequency components that complicated accurate measurement with limited bandwidth. Power transferred through the traction power bus is more practically measured than at the motor shaft or motor input. This is approximately "DC", although the inverter switching frequency of up to 45 kHz and the rise and fall times on individual SiC MOSFET modules are typically a fraction of a microsecond when low gate resistance is featured in the design. The high frequency effects on the DC bus do not contribute much of the power transfer, so low frequency telemetry of the output voltage and current from the battery control modules and the input voltage and current to the cruise motor inverters were consistent with each other since the losses along the bus were minor. As both the battery control module and motor inverters were experimental hardware, the system also included independent voltage and current sensors in the contactor pallets that drove cockpit instrument panel displays so that the pilot would reliably have insight into the power levels in lieu of traditional engine instruments. The sensor measurements were also telemetered and recorded by the research instrumentation system for real time monitoring and post-test analysis.

The most substantive change to the traction architecture after the critical design review was the addition of an external disconnect feature. As the project team improved the fidelity of the requirements for daily operations and identified failure modes in the aircraft system or in the procedural controls, it became clear that an additional means to disconnect traction power being transferred from the onboard battery packs to the inverters and motors would be needed. This was a simple change as the cockpit already has switches controller high power contactors in the battery control modules for this purpose, so the switch wiring was routed through a loopback connector externally accessible behind the cabin. Even if a hard landing or other event prevents the pilot from being able to switch off the battery system contactors, external crew or emergency first responders could cut the low voltage loopback wires and the spring-loaded contactor would revert to the normally-open state and disconnect the battery packs from the traction power distribution bus. This feature was also useful as a secondary means to secure the traction power bus and could even have been used to remotely enable and disable the bus for automated ground testing without an aircraft operator sitting in the cockpit.

3.1 Battery System

The X-57 battery system was expected to be a relatively simple packaging activity to map the energy storage capability of commercial, off the shelf lithium-ion battery cells to the high voltage, high current configuration needed for the X-57 flight profile. The X-57 mission profile estimation drove the selection of the Samsung INR18650-30Q cell as a good combination of both specific energy and power rating.

3.1.1 Initial Battery Design

The initial packaging design was based on the currently published best practices for cell mechanical spacing and included an air gap of several millimeters between each cell. This design included provisions for full gas and particulate containment with pressure equalization via a synthetic permeable membrane on a custom vent (permeable vents would later become a standard, off the shelf product but were not yet available). Membrane selection was proven to be incorrectly sized during cell runaway and propagation prevention testing as it failed to either equalize pressure fast enough or burst (both of these are features of current products). This design also required complex cooling features to reject heat produced in the cells during operations since the sides of the cell cans were in free air.

Testing the response to thermal runaway of a cell and the likelihood of propagation of runaway to neighboring cells was achieved by wrapping sacrificial cells in nichrome wire and directly heating the cylindrical cell can on a partially populated module (320 out of the designed 640 cells). This air-gapped battery pack design failed to prevent cell-to-cell thermal runaway and resulted in a total runaway of all 320 live cells. The pack did not contain the flame or ejecta and had an initial flame escape within seconds of the runaway propagation, continuing to burn for several hours.

3.1.2 Battery Packaging Redesign

An unplanned battery packaging development effort was added to the project activity to study how modern commercial cells could be safely packaged and what packaging mass and volume overhead penalties would result. The redesigned pack was required to operate with high reliability and not present a fire hazard to the aircraft or crew in the event of a cell thermal runaway. The National Aeronautics and Space Administration (NASA) had been developing battery pack designs for various human spaceflight applications that embed cylindrical cells in a heat dissipation block while also shielding cells from the flame and effluent of a failed neighboring cell [8]. Extending this design architecture to a higher voltage and higher current configuration required substantial iteration on the cell-to-block clearance (bore size) to get the right balance of expansion volume and neighboring cell heat absorption without inflicting enough thermal or mechanical stress on neighboring cells to cause a runaway propagation. A

key feature of this approach with cylindrical cells is for a runaway cell's thermal load to be absorbed by healthy neighboring cells at a controlled rate such that additional thermal mass and dissipation material is reduced while ensuring that the healthy cells are not overloaded. This redesign also incorporated individual cell fusible links etched into the nickel bus bar at the cathode of each cell. This was a feature that had been demonstrated on the NASA human spaceflight designs and is described in a subsequent activity to develop a reference high power Li-ion battery [9]. It requires some custom tuning based on the bus configuration and the series/parallel architecture of the pack but effectively mitigates some cell failure modes (e.g., internal short circuit if there is enough parallel cell current available to trigger the fusing).

During this redesign process, it also became clear that the battery storage modules with 640 cells and integrated disconnect switches would have too much packaging overhead and would be too heavy to be handled safely (these were trending toward around 110 to 120 lb). The packaging architecture was split so that each module would hold 320 cells in a 20p16s configuration (blocks of 20 cells in parallel connected in series strings of 16 blocks), thereby doubling the number of modules and halving the individual weight. With 16 modules on the aircraft, it was no longer practical to install a disconnect switch into each module, so string disconnects were added to the battery control module.

Module design testing included thermal, random vibration, mechanical shock "proto qualification" which is testing in environments that exceed the operational environment, but not so extreme as to substantially reduce the life of the test article in lieu of a full design qualification approach with dedicated qualification test article. As a result, the qualification test article can still be used as flight hardware either as a spare unit or as the primary vehicle hardware which reduces the overall production quantity and therefore the cost and schedule required for production. This trade-off for the reduced cost of a couple hardware units in exchange for less demonstrated design margin is attractive for prototype and experimental activities like X-plane development but would not be as suitable in a production activity. Figure 6 show the elements of the design qualification test program.

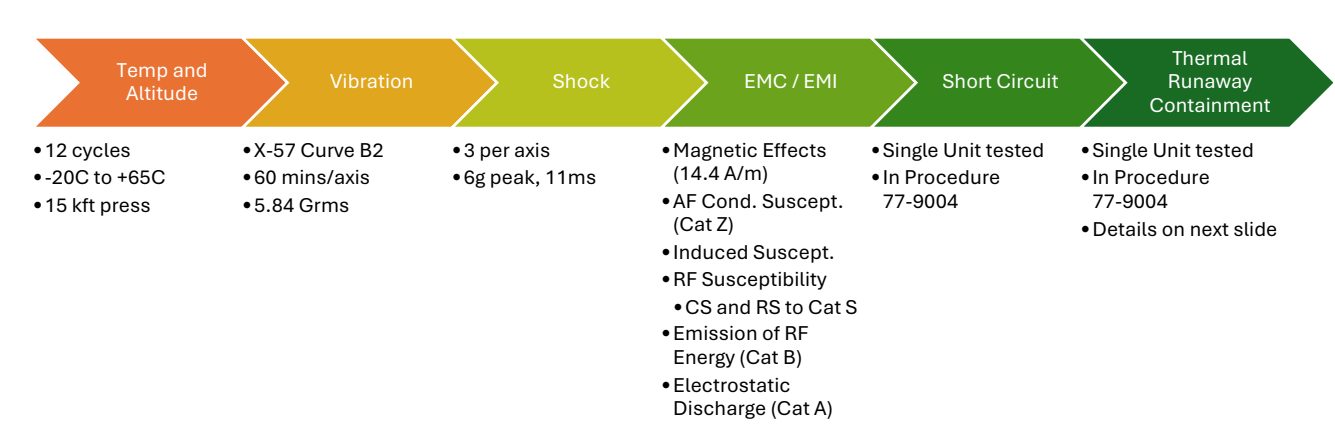


Figure 6 - Battery Module Qualification Test Program

Each flight module completed environmental acceptance testing for both mission reliability demonstrations and workmanship quality assurance. The testing also included Electromagnetic Interference/Electromagnetic Compatibility (EMI/EMC) qualification, short circuit testing, and an updated thermal runaway containment and propagation prevention test. This updated thermal runaway test could not use the cell can heating trigger because the passive thermal dissipation of the new pack design would effectively absorb the energy. Instead, cells with internal short circuit devices were installed in place of the corner cells in a test article. This short circuit device would fail reliably at an internal temperature of approximately 70°C instead of the typical runaway threshold of over 120°C. By

rapidly charging and discharging the trigger cell while maintaining maximum credible operating temperature for the rest of the pack, a realistic runaway event with worst-case energy could be produced. Three of these events were successfully demonstrated with no neighboring cell runaway and total containment of the flame and venting of the cell runaway products [10]. The elements of the module acceptance test program are shown in Figure 7.

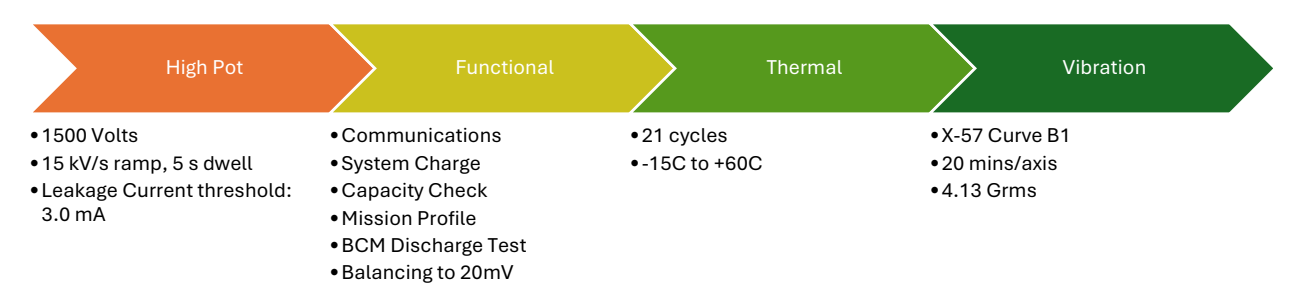


Figure 7 - Battery Module Acceptance Test Program

3.1.3 Battery Control Modules and Lockout/Tagout Boxes

The BCM for each battery pack was responsible for cell voltage and temperature monitoring and telemetry, distribution of the traction power, sourcing of avionics power, discharge current monitoring, and charge control and monitoring.

The traction power distribution feature was what enabled the external disconnect capability for ground crew and first responders. The main contactor system in the BCM is remotely controlled by dry contact and sequences positive and negative main contactors interleaved with a smaller precharge contactor. This automatic control compliments the manual disconnect switch in the Lockout/Tagout (LOTO) box.

The LOTO Box also provided an inline fuse used to limit the exposure of the ground crew from arc flash during installation and maintenance of the battery modules and for protection of bus faults during operation. These two drivers for the fuse system were marginally compatible as the personnel protection feature requires a lower fuse rating than the nominal operating sizing calculation with thermal margins included. When the power required for a reference mission is modeled with battery voltage dynamics [11], the current level exceeds 175 A during takeoff and remains at around 150 A during climb and cruise since voltage is dropped as the power requirements are also dropping. Figure 8 shows the battery current predicted by this model for the reference mission overlaid by the measured current during a mission profile test with the aircraft battery system discharge with the same power levels and durations. This response was slightly conservative as demonstrated by testing of the battery packs with the same power profile while monitoring voltage and current. The fuse rated at 200 A was slightly undersized for these loads at the temperature range that could be present in the cabin, but a larger sizing would not have provided sufficient arc-flash protection during maintenance activities. This mismatch was more severe for reference missions that included the high lift motor loads, but the selected fuse may have enough allowance given the margin in the thermal models in those cases as well. The loss of traction power in flight due to a blown fuse or other failure in the experimental powerplant was considered in the project hazard analyses. The flight test plan provided the capability to glide to the runway throughout the planned flights [12].

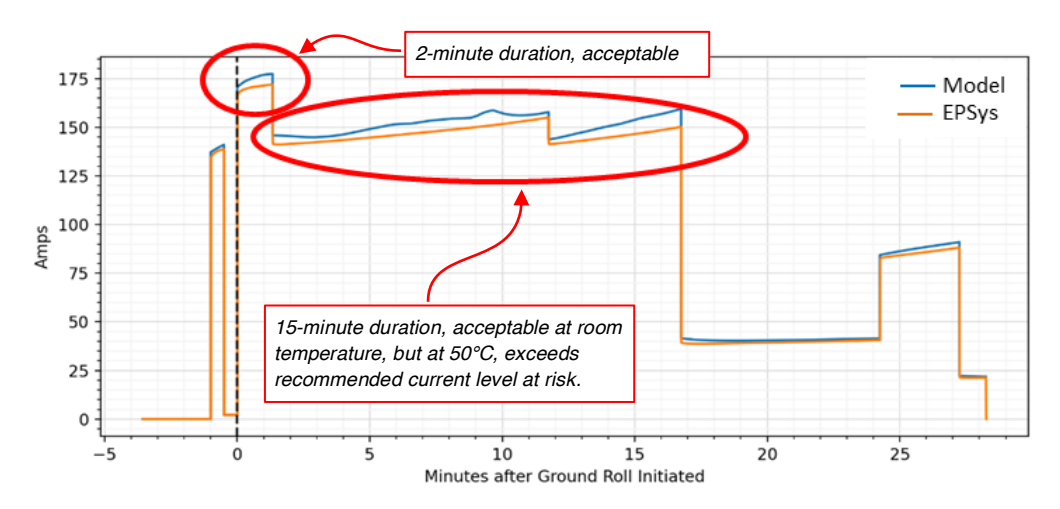


Figure 8 - Traction Battery Current for a reference mission (model data and ground test data)

Avionics power for the aircraft systems is supplied by a system of DC/DC converters that accept battery module terminal voltage from half-packs (four battery modules; 190 to 270 V) and produces 13.8 V at up to 70 A as shown in Figure 9. The DC/DC converters were independently enabled by dedicated cockpit switches and their operating status indicated in the cockpit audio system and cockpit annunciator display.

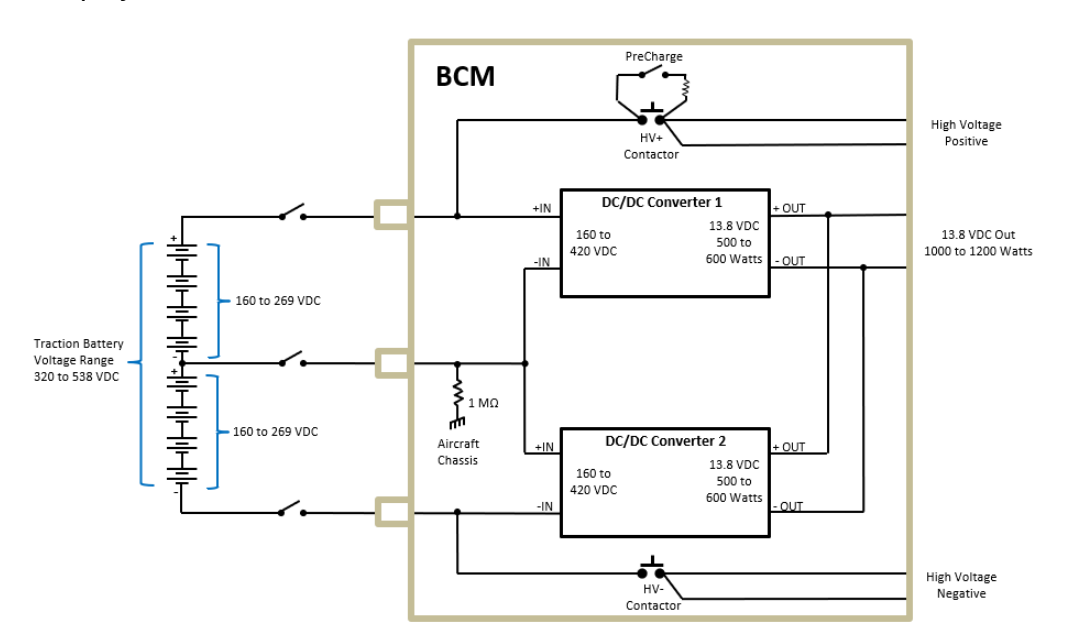


Figure 9 - 13.8 V Power Supplies

The Battery Control Module had an Isolation Detection Unit (IDU) feature that constantly tests electrical isolation between the high voltage bus and the aircraft's aluminum structure. This capability was instrumental in analysis of the shock hazard that could result from the floating traction system contacting aircraft structure or another system and presenting a touch hazard to the air or ground crew. This resulted in a more robust system design that could continue to operate in the event of a single isolation fault (the system ceases to float) while still alerting the crew that there could be a hazardous condition until the battery is disconnected. This was a challenging feature to implement as each battery pack was independently probing for isolation faults through a current limited scanning sequence between each battery pack terminal and the vehicle ground, so if a test configuration caused the two packs to share a return (e.g., when powered by a multi-channel, common return power supply) then the scanning

sequence would occasionally overlap between the two packs and falsely indicate a fault. This also happens in facility powered configurations (e.g., battery charging) if the ground support equipment has its own isolation detection system.

The battery system design includes monitoring of all cell voltages (one measurement for each block of 20 parallel cells since they are electrically bonded) and two temperature measurement for each block of 20 parallel cells (256 measurements per pack). The BCM collects the values from each of the cell monitoring boards embedded in the battery modules then telemeters each of the values out in Command Bus messages. It separately reports summary voltage and temperatures along with pack current and overall BCM health and status on additional Command Bus messages, which are used for summary display in the cockpit multifunction display. All the BCM command bus message data is also collected by the instrumentation system to be recorded in the onboard flight data recorder and downlinked to control room.

The configuration control of the battery system codebase was divided into two parts. First, a Complex Programmable Logic Device (CPLD) managed the digital logic and fanout for contactor control and annunciator multiplexing directly in hardware logic. Second, the Battery Management System (BMS) Software package was developed to NASA Class 1S processes to provide high assurance for monitoring of cell and system sensors as well as alerting when limits exceeded via both cockpit annunciation and telemetry messages. The BMS did not have any control of the battery pack discharge mode (contactor logic was isolated to the CPLD) meaning the pilot could choose when to enable or disable the system based on battery health in conjunction with aircraft state. It could, however, interrupt battery charge operation if cell voltage or temperature limits exceeded safe values.

3.1.4 Battery Control System Testing

The battery control system (the BCM and LOTO boxes) we comprehensively tested by the manufacturer (Electric Power Systems, Logan, UT, USA) individually and with a flight battery string to verify and validate the system design. This included proto qualification of a representative unit and acceptance testing of all flight hardware which built up to a full subsystem mission profile test with representative discharge and recharge power levels through a fill operational cycle.

This testing was split into a five-phase sequence of test cases that methodically verify each of the system and subsystem requirements on the battery control system and validate the overall design and implementation before delivery to accelerate any modifications that were identified during testing (Figure 10). The build-up testing at the interface and assembly levels for each component met the vehicle environments defined per the X-57 Environmental Test Plan (ETP-CEPT-007) including specific requirements for thermal, random vibration, and shock acceleration for each zone of the aircraft. The final phase of the test program included integrated tests with a flight battery pack and full power charge and discharge profiles to match a reference aircraft operational sequence. A full documentation "end item data package" was collected including the complete system design, analyses, as-run test procedures, qualification procedures, certificates of conformance, deviations, waivers, non-conformance reports, and test results for the entire test program.

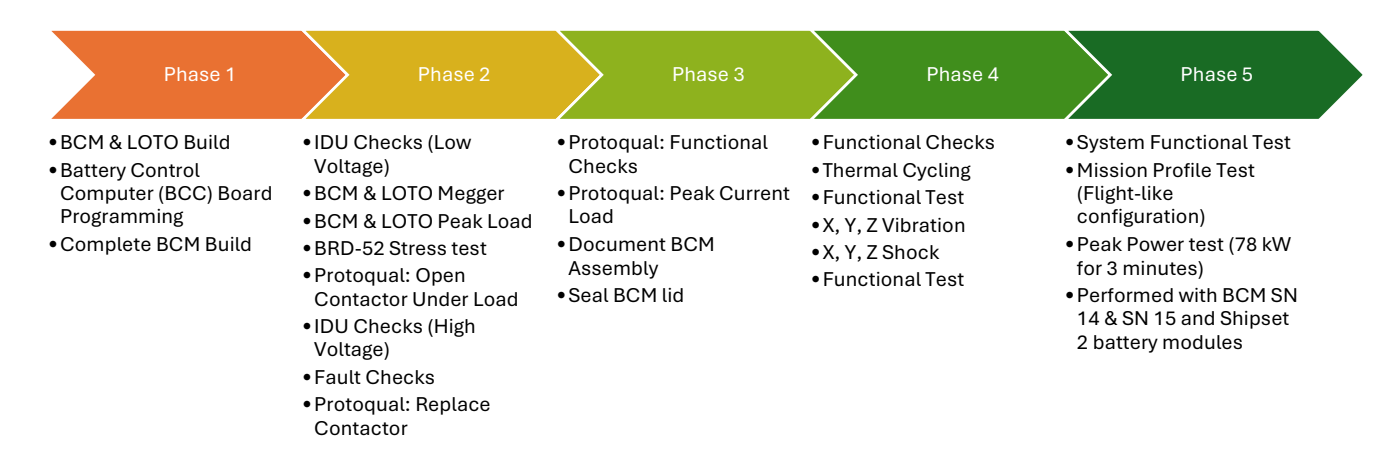


Figure 10 – Battery Control System Test Program

3.2 Cruise Motors

The cruise motors (CMs) are dual-winding, three-phase, air-cooled, out-runner electric motors custom designed for the X-57 Maxwell by Joby Aviation [13]. These motors operate with inverters at 461 V nominal, providing 72 kW peak power to the propeller at 2,700 RPM and 60 kW continuous power at 2,250 RPM. These motors directly drive the propellers and provide primary thrust for the X-57 Maxwell airplane. Each of the independent 3-phase windings in the CM is driven by a sensorless inverter called a cruise motor controller (CMC). If a single CMC becomes inoperable, the remaining operational CMC for that motor can be commanded into overdrive such that the active winding deliver up to 25% power over its nominal rating for a short time. For Mod II, the electric motors were located within the stock Tecnam P2006T nacelle locations [14].

3.3 Cruise Motor Controllers

The CMCs were originally designed by Joby Aviation and QDESys (Verona, Italy). The initial design was unable to pass vibration screening tests and the CMCs were redesigned by the NASA with assistance from X-57 prime contractor Empirical Systems Aerospace (ESAero) (Empirical Systems Aerospace, Inc., San Luis Obispo, CA, USA), reusing some of the original boards. The CMCs convert DC power from the traction battery systems into 3-phase AC power providing torque control over the X-57 cruise motor. The CMCs use a sensorless field-oriented control (FOC) inner loop to maintain commanded torque control across a range of speeds, traction bus voltages, and operating conditions. The CMC is composed of five custom-printed circuit boards (PCBs) outlined in Figure 11.

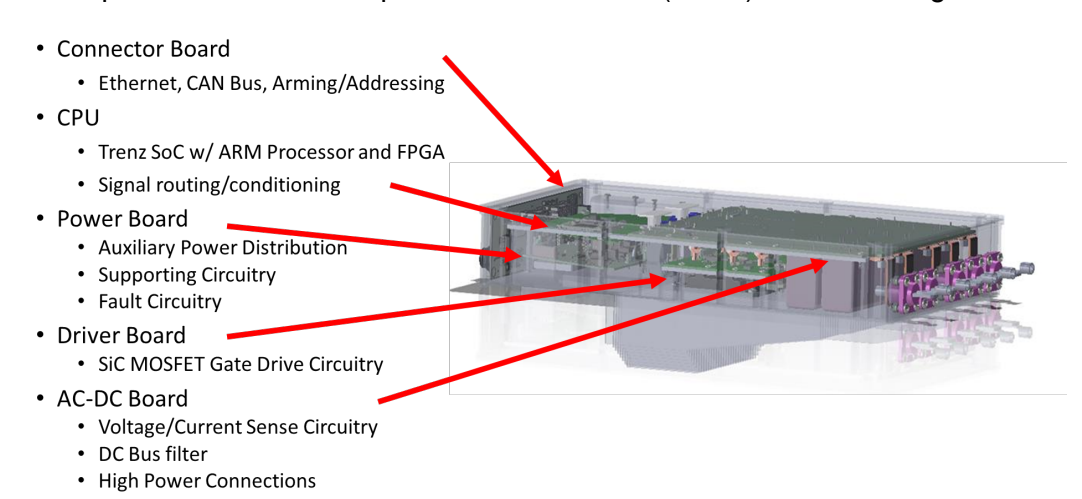


Figure 11 - Cruise Motor Controller Packaging

The normal operating voltage for the X-57 traction bus was between 320-538 V. In nominal conditions the peak output power per CMC was 36 kW at 2,700 RPM. In the case of a CMC failure, the remaining CMC could provide up to 45 kW in an overdrive scenario. Each CMC used three silicon carbide (SiC) half-bridge MOSFET modules to convert between DC bus and motor winding power.

The CMC used the Trenz Electronics TE0720 system-on-a-chip motor-control field-programmable gate array (FPGA) IP-core (Xilinx XC7Z020). The FPGA field-oriented controller image was designed by QDESys, and a separate outer-loop CPU executive application layer was developed at Armstrong Flight Research Center (AFRC). CAN Bus communication was used for torque command input and telemetry output. Ethernet communication was used for software maintenance. The interfaces and relationships between the CMC hardware and software elements are described in Figure 12.

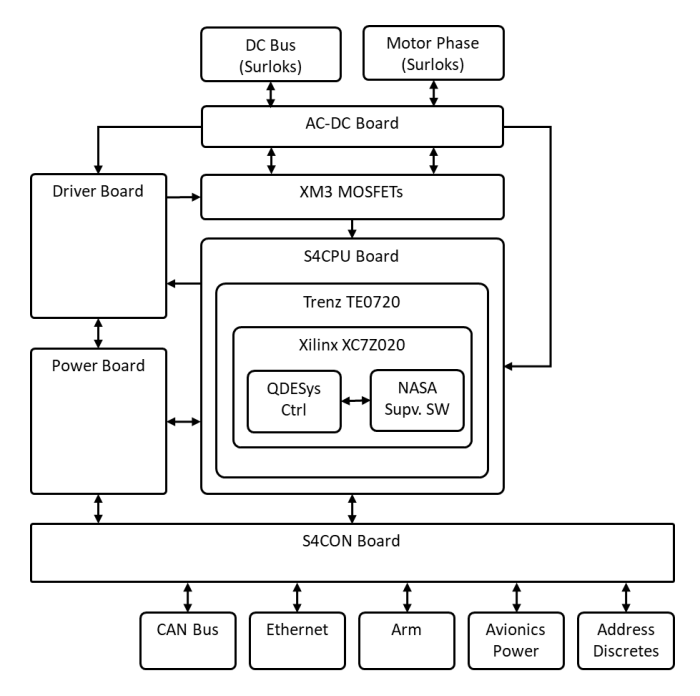


Figure 12 - Simplified CMC Internal Interface Diagram

The key design features of the cruise motor controllers include:

- Achieve a minimum of 97% efficiency at relevant speed, torque, and power settings using a high-power Silicon Carbide (SiC) MOSFET-based motor drive
- Survive the thermal environment within the X-57 Mod II nacelle with passive air-cooling
- Pass the acceptance and proto-qual test program per the X-57 Environmental Test Plan

The original CMC design relied on three (one per phase) Wolfspeed CAS300M12BM2 62mm half-bridge MOSFET "BM2 modules" to convert the DC power input to 3-phase AC power output to the CM. Environmental testing showed that these modules could not withstand the original acceptance level vibration environment defined by the project (random vibe 7.7 G_{RMS}, 20 min/axis). A presentation detailing the failure modes of the BM2 module and the initially proposed solutions is available [15]. Upon further analysis of the CMC design the project also found deficiencies in the internal current sense circuit architecture, half-bridge MOSFET module gate drive design, and in the heat sink/thermal design. Additionally, the original design was found to have unacceptably high levels of DC Bus voltage ripple, roughly 40%. The controllers and the Cruise Motors were initially treated as commercial/off-the-shelf by the project with the expectation that the Technology Readiness Levels (TRL) of these items were high. The plan was to quickly test and qualify them for flight, but the deficiencies found in the design

(detailed in [16]) required the project to pivot and redesign the CMC to implement fixes in the following areas:

- 1. Replaced original MOSFET modules with Wolfspeed SiC 400 Amp XM3 modules. The updated modules had improved electrical and thermal performance, as well as a more robust packaging scheme. The advancement in packaging between the BM2 series modules and the XM3 series was critical to the retrofit effort. The volumetric power density of these devices is effectively three times better and could be adapted to fit in the same CMC case (Figure 13).
- 2. DC Bus and motor winding current sensor replacement. Modified analog signal design on circuit boards to improve signal integrity and changed packaging layout of CMC to better colocate sensor and transceiver without a noise source between. The goal being to improve the signal-to-noise ratio and reduce error in the current feedback control loop.
- Aluminum case with integrated heat sink designed to fit 1-for-1 swap with the previous CMC design. Addresses the observed vibration testing shortfall of old design through internal support of the PCBs and overall stiffened design.
- 4. Improved CMC heat sink design to lower CMC enclosure-to-air temperature delta. The updated MOSFET package also has a higher junction temperature limit than the original.
- 5. Isolated low-power PCBs from high-power MOSFET sink, and cool via enclosure backplate exposed to cooler (near-ambient temp) flow, via aux inlet or natural circulation in nacelle.
- Redesigned an optically isolated gate drive circuit, relocated directly on top of the MOSFET
 modules to reduce parasitic parameters and improve drive quality. The driver also included a
 hardware desaturation fault circuit to protect the MOSFETs against over-current events.
- 7. Included improved DC bus filtering with a cascading network of filter capacitors.

The XM3 CMC redesign included multiple prototypes and used a trial-and-error based testing approach to arrive at a flight worthy product. Three revisions of the prototype CMCs were created before the project was satisfied with the design and performance of the inverters.





Figure 13 – Cree/Wolfspeed Half-Bridge SiC Power Modules Left: CAS300M12BM2 ("BM2") 1200 V, 300 A, 4.2 m Ω ; Right: CAB400M12XM3 ("XM3") 1200 V, 400 A, 4.0 m Ω

3.4 High Lift Motors and Controllers

The high lift motor controller (HLMC) was designed as part of a distributed electric propulsion architecture which included two Cruise Motors (CMs), each controlled by two CMCs. The CM system was complemented by twelve HLMCs each controlling a high lift motor (HLM) and high-lift propeller (HLP). An artist rendering of the aircraft can be seen in Figure 14. The HLMCs were to be used for boosts in takeoff and landing and would not run during normal cruise operations. Each HLMC was required to be passively cooled without interrupting the outer mold line of the nacelle, weigh 1 kg, use

the same traction bus as the cruise motors, and produce a greater than 97% efficient AC output to the three-phase HLM providing 24 Nm of torque. The efficiency requirement is essential to bound the thermal design of the high lift nacelles, so it became apparent that it was more effective to treat this as a thermal loss limit of 330 W effective at all operating modes. This allows the design to be optimized for the high-power case but doesn't pose unneeded constraints on the lower-power operations such as low speed startup states when the absolute efficiency is lower, but not critical. The HLMC team approached this challenge by using fast-switching discrete SiC MOSFETs. The high-speed switching led to high efficiency of the inverter, which was measured at 98.3%. The discrete SiC FETs were necessary to meet the restrictive mass requirement and achieve the efficiency needed to use strictly passive OML cooling. The complete HLMC design presented in this paper includes a microcontroller, three-phase power inverter, and ground and flight software. [17]

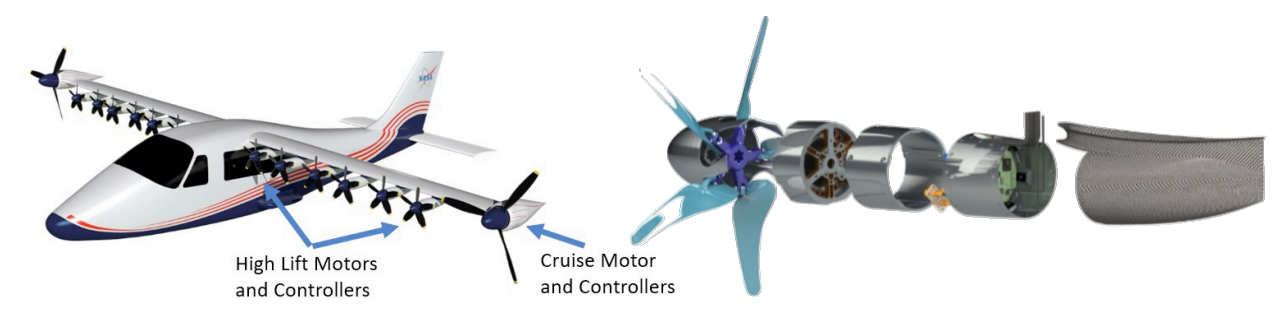


Figure 14 - Left: X-57 in Mod IV configuration, Right: High Lift Propulsor Assembly (incl. propeller, motor, and controller)

Major electrical components in the HLMC include input filtering to reduce DC bus ripple to the nominal lithium-ion battery traction bus and a three-phase inverter to drive the high lift motor. For the inverter, Silicon-Carbide MOSFET switches were chosen for their high operating temperature, high voltage capability, and low parasitic capacitance which allows for the potential to maximize the efficiency of the inverter through the rapid switching transitions. The MOSFETs are driven through optically isolated driver circuits. The driver circuits are the interface between the power train and the control circuits. The link to the control circuits is established through a fiber optic Ethernet interface to the control computer in the laboratory, or the avionics computer on the X-57 vehicle. Input commands and control algorithms are processed through a Texas Instruments Delfino microprocessor. The Delfino was chosen because of its programming capability through MATLAB and Simulink which enable rapid prototyping via code generation using visual and interpretable function blocks.

The controller software and control parameter development strategy were optimized to boost efficiency over standard practices. A FOC strategy is used to control the speed of the motor. The variant of FOC used in this controller is derived to demand the minimum current required for stable operation, as opposed to other FOC variations which use more current to accomplish other control objectives. In addition, discrete space vector, pulse width modulation is used, which eliminates some of the MOSFET switching losses.

3.5 Qualification and Acceptance Testing

The X-57 project developed an airworthiness acceptance test program that each CM and CMC would be required to pass to be considered flight qualified. The main components of the airworthiness acceptance test program included environmental testing (thermal and vibration), powered dynamometer testing, and on aircraft Verification and Validation (V&V) testing. The project developed individual CM and CMC Test Plans (TP-CEPT-015 and TP-CEPT-013 respectively) as a supplement to the project's Environmental Test Plan (ETP-CEPT-007) and V&V test plan (TVP-CEPT-006). These

and other project documents are being reviewed and may be available for release to partners, other agencies, and, in many cases, the public via the NASA Technical Reports Server. The majority of CM and CMC tests would be completed on a dynamometer test stand built by the projects prime contractor Empirical Systems Aerospace (ESAero).

3.5.1 Cruise Motor Controllers

Upon delivery each circuit board was required to pass an individual board test developed to screen for workmanship defects. All necessary components were then provided to the instrumentation fabrication shop at NASA AFRC for assembly of the flight controllers. A detailed assembly document was written by engineers along with technicians to ensure each build was assembled with the same approach. Multiple inspection points by quality assurance and engineers, including multiple hi-pot isolation checks, helped reduce the likelihood of build errors and a need to reopen the CMCs after assembly. Post assembly, the CMCs would be powered on and tested at low power with an unloaded cruise motor to ensure proper functionality.

The controller was then required to complete a series of high power and temperature tests on the dynamometer to ensure they met all performance metrics required for flight [18]. These tests proved the CMCs could perform for the required flight durations at the maximum power levels with margin. The high MOSFET temperature tests gave insight into the controller drive circuit and allowed for electrical performance characterization between units. Additionally, two CMCs were tested at higher power levels, or proto-qual levels, to ensure there was margin in design. The CMCs were also required to complete environmental screening tests including vibration and thermal chamber testing [19]. The controllers could then be used as flight units on the aircraft to conduct ground operations, and eventually verification and validation (V&V) testing of the entire powertrain and all flight interfaces within the X57 aircraft. The project closed out before V&V testing was started. The elements of the CMC qualification and acceptance tests are shown in Figure 15).

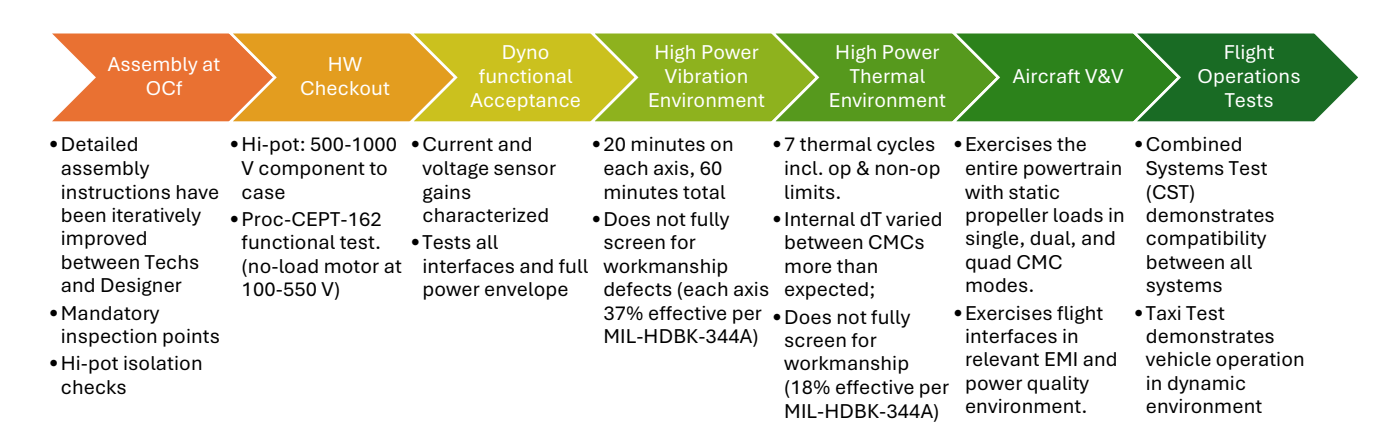


Figure 15 - Cruise Motor Controller Qualification and Acceptance Test Program

3.5.2 Cruise Motors

The Cruise Motor stators and rotors were manufactured by Joby Aviation and assembled at Empirical Systems Aerospace. Airvolt, a single propulsor test stand built at NASA AFRC [20], was used to complete endurance testing on the Cruise Motors per Federal aviation regulations (FAR) Part 33 Airworthiness Standards: Aircraft Engines Test Objectives. FAR Part 33 was selected because a flight qualification standard for electric motors did not exist at the time, and it was the existing standard used by NASA. The Cruise Motor testing objectives on Airvolt included endurance and vibration testing, collection of torque, thrust, power, and efficiency data for performance, and to identify any potential

hardware deficiencies. On aircraft ground operations were also conducted at Scaled Composites (Mojave, CA, USA) during this time. Following the discovery of assembly and design defects, in the bearing installation and stator winding and chassis electrical isolation respectively, the Cruise Motor stator was redesigned, and a new batch of motors was assembled. The Airvolt test stand was abandoned due to difficulties achieving long run times from a lack of sufficient motor cooling, as well as the original CMC design being unreliable. All subsequent airworthiness testing would be conducted on the dynamometer test stand at ESAero.

Stator DC Injection, as well as insulation resistance tests were completed prior to the CM being mounted on the dynamometer. Once mounted, the dynamometer load motor would spin the unpowered CM so that the back-EMF signature could be measured, certifying acceptable permanent magnet health, as well as the CMs proper assembly. The subsequent powered tests would ensure that the motor could achieve the maximum power, torque, and durations to meet the flight objectives with margin. One cruise motor was also required to perform at elevated test levels and duration (proto-qual including altitude and thermal chamber testing) as well as complete additional qualification testing, which included a thermal envelope expansion test running the stator windings near their maximum limits and ended with a destructive teardown inspection.

Throughout the CM acceptance testing campaign and on-aircraft ground testing, multiple discrepancies in the design, especially in the bearing type and housing, were found. Solutions, mitigations, and redesigns were explored several times throughout the project lifespan, but eventually the design was deemed non-flight worthy by the team, unless major stator redesigns were enacted. The project closed out before the redesign could be developed. The following test plan (Figure 16) includes the original airworthiness test approach, along with some proposed updates (highlighted) that the team believed could have helped to vet the design more stringently, although the updated approach was not fully defined before project closeout

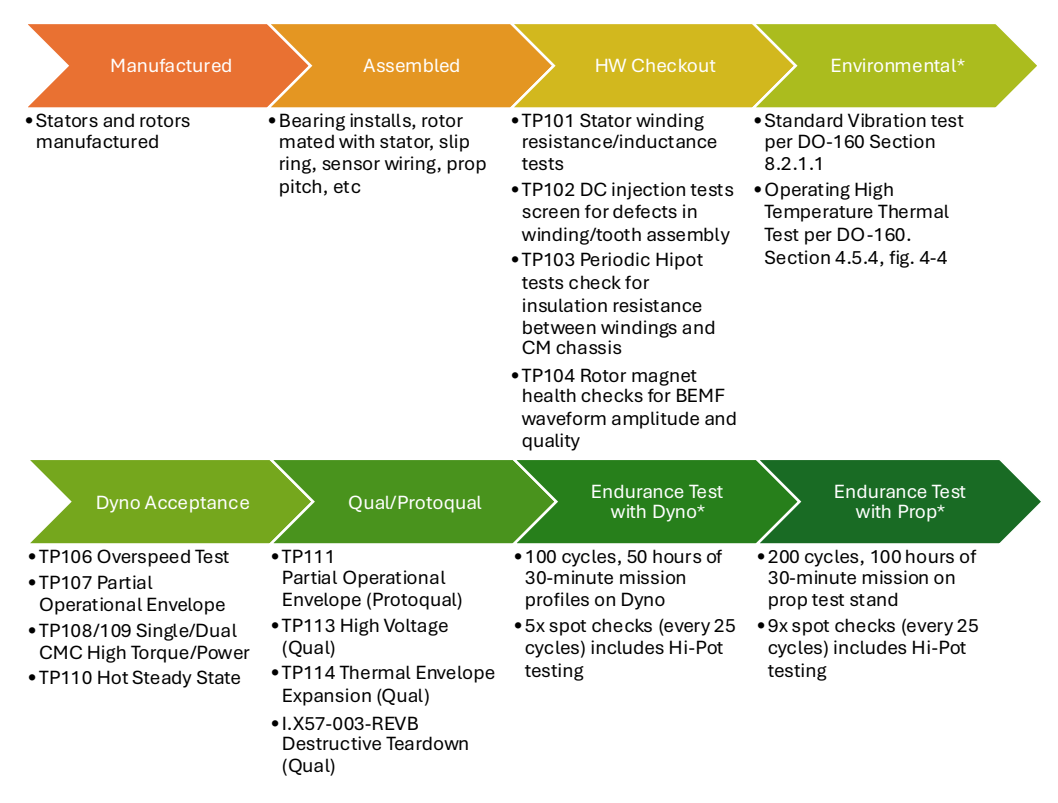


Figure 16 - Cruise Motor Qualification and Acceptance Test Program
*Note: Environmental and Endurance Tests were in-work but not fully defined prior to project closeout

3.6 Integration and Electromagnetic Compatibility

The CM and CMC qualification and acceptance testing took place almost exclusively off the aircraft. Although some minor EMI effects were discovered and resolved during the revision and prototyping process of the Cruise Motor Controllers, the high-powered dynamometer acceptance and qualification testing, which used power supplies and not the X-57 batteries, did not produce any EMI concerns. Once qualified, the CMs and CMCs were used for on- and off-aircraft testing. The X-57 team used an off-aircraft hardware in the loop (HIL) testing strategy to initially test the full X-57 powertrain, including the X-57 batteries, battery control modules, contactor pallet, cruise motors, and cruise motor controllers. In this configuration it was found that critical data on the batteries Isolated Serial Peripheral Interface (ISOSPI) was being lost immediately upon arming of the CMCs to send power to the motors.

The CMCs operated at switching frequencies near 40kHz, and with the use of SiC MOSFETs with fast turn-on/off transition times, the EMI generated from these switching events was large enough to interfere with sensor and communication lines in multiple aircraft systems. The noise generated by the switching events was a known issue and the DC bus voltage ripple of the original CMC design was brought down from 40% to below 5% in the flight version of the XM3 CMC design. This was accomplished through a cascading network of filter capacitors, but a common mode choke was not implemented before the CMC design was finalized and flight units built.

The root cause of EMI and loss of critical data was due to CMC switching events (square wave pulses were "riding" on top of AC waveforms going into the motor and propagating back from the inverter to the battery pack due to coupling capacitance). EMI is represented as a common mode current which finds a path to sensitive electronics disrupting regular operation causing dropouts, shutdowns, etc. This would propagate from any copper connections out of the CMCs (traction or avionics) through capacitive coupling between subsystems and back through low impedance paths. A common mode choke can be used to impede common mode current and attenuate high-frequency noise. Implementation of Pi filters (capacitors and inductors) yielded the best results in simulations and were successfully tested on the off-aircraft HIL configuration. Custom soft core magnetic material inductors were produced in-house at NASA Glenn Research Center and combined with capacitors chosen for their low equivalent series inductance (ESL), to create a T-type inductor/capacitor (LC) filter that was placed on the traction bus cables as close to each CMC as possible (Figure 17). Each controller had a matching T-filter. An additional 20 common-mode chokes were used across X-57 communication and sensor harnesses to reduce EMI effects. In the future, it is recommended that a common mode choke on the DC bus input be integrated into the inverter design, and a full test of the aircraft powertrain and relevant subsystems be completed before the inverter design is finalized.



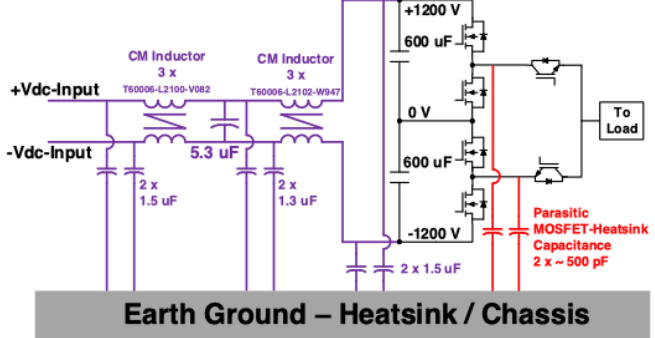


Figure 17 – Custom T-filter (LC, lowpass).

Left: flight unit packaged for inline DC bus installation., Right: filter schematic in relation to reference inverter.

4 Command System

The Command System for Mod II and III developed per the originally published architecture performed well in developmental tests and in integrated aircraft configurations. Details on the system as implemented are available in [21]. The architecture shown in Figure 3 is nearly the same as the layout presented during the systems design phase with two changes: the removal of message-controlled relays and the addition of ground support equipment (GSE) interfaces.

The CAN Bus message-controlled relays were removed from the design since the cockpit systems that would be required to react to the Command System events was limited to annunciation as all cockpit systems are pilot controlled. This design choice further simplified the requirements on the Command Bus by removing any safety criticality dependency on the bus data. This led to a design choice to develop the software in the CMCs to a level that would guarantee a reliable reversionary mode if the CAN Bus messages were corrupted or missing. The only messages that the CMCs were monitoring from the Command Bus were the throttle lever encoder positions that communicated the desired motor torque setting from the pilot. The CMCs were designed to maintain the motor state in the absence of valid messages so that the pilot would have continuous propulsion available at the current system levels until manually disarming the CMC for an orderly shutdown. The throttle lever encoders that were selected and integrated into the system were Baumer BMSV 58K1N 24R 12/00 C0N units. These have redundant sensors on the rotary position, so the CMCs were able to compare the position values from the two sensors and automatically identify and recover from a failed sensor.

Additional GSE interfaces were required for system verification and validation to collect message logs and verify timing statistics. The GSE interfaces were instrumental for vehicle integration tests as well as the CMC software validation conducted in the integrated systems require real-time throttle control and telemetry evaluation by the flight systems development and integration team described in detail in [14]. This interface was additionally used for battery system integration checkouts and enabled real-time monitoring of cell charge state during ground charge and discharge tests.

Several MoTeC-branded products were incorporated into the Command Bus: a multifunction display, a display controller, and remote data acquisition modules. These are not intended for aircraft application, but testing demonstrated that they were reliable and rugged enough for non-critical data collection and indication and were used for pilot situational awareness and for ground test support.

The fiber-optic bus extenders were an essential enabling technology for the CAN Bus design. The risks of EMI and lack of EMC with the experimental cruise motors, controllers, and battery system were a driver for the overall Command Bus network layout. Given the floating, isolated traction power architecture and the CAN Bus that would span between each of the CMCs, BCMs, and other aircraft systems, electrical isolation was required to be integrated into the network. The Western Reserve Controls (Akron, OH, USA) WRC-CANR-NEM-DF device was selected as the basis for a custom product that would be developed for the X-57 aircraft environments. The repackaged, ruggedized flight configuration is shown in Figure 18. The key feature of this device was the intelligent store-and-forward buffering capability that would automatically negotiate the CAN Bus message priorities at each end of a fiber optic link to each of the CMCs from a main, central bus segment. As there were not real-time timing requirements on the Command System messages, this was an ideal solution that allows for each of the remote bus segments to be locally coupled to the traction system devices without compromising the overall isolation.





Figure 18 - Custom fiber optic bus extenders ruggedized for aircraft environments.

Left: main bus segment FOBE; Right: cruise nacelle FOBE

An unintentional side effect of this architecture that was a consequence of the throttle lever encoders and CMC design features was that the throttle lever encoders did not have the capability to automatically transition to operational mode so that periodic position messages are transmitted automatically. Instead of adding an additional CANopen manager device, the CMCs were designed to send the network management start commands if the throttle position messages were missing from the bus. Unfortunately, because each CMC was independent, when a throttle lever encoder needed to be commanded to start, multiple CMCs would be sending the same network management message with CAN Bus Arbitration ID of 0x000. When messages with the same arbitration ID can originate from multiple devices on a CAN Bus, the message arbitration feature is compromised. In the X-57 Command System, this can result in bus segments with two devices installed (such as the CMC LB or CMC RA segments each with only a CMC and a FOBE). If a CMC is encoding the network management message at the same time the FOBE is relaying the network management message it collected from the central bus segment, then neither device will detect the collision, and no device will acknowledge the bus activity, so the local segment will get stuck in a loop while each device continuously retransmits the unacknowledged messages. To address this, the FOBE firmware was modified to mask message ranges that could have redundant sources so that those messages were not transmitted to the remote bus segments but would still be delivered to the main bus segment for receipt by the throttle lever encoders.

The Command Bus for the High Lift System in Mod IV was implemented as an Ethernet network instead of further extending the CAN Bus used for the cruise motor controllers and the battery management system. This separated the requirements and their associated verification and validation for each of the vehicle configurations and accelerated development. The primary interface for the pilot to the high lift system is via discrete switches and annunciation and an associated combinatorial logic distribution network. The digital bus messages that were needed in this design were air data measurements from the pitot and static pressure sensors. This allowed for a completely distributed architecture with no centralized controller (or point of failure) needed to prescribe lift augmentation setpoints. Instead, each of the high lift motor controllers could independently determine the appropriate operating mode (discrete inputs and health checks on digital inputs), calculate airspeed and altitude, and target the intended motor speed based on these factors [22].

5 Avionics Power System

The Mod II avionics power design is based on the stock Tecnam avionics power architecture which uses three 12 V power sources, a battery, and two alternators to provided redundant avionics power. This redundancy was preserved in the X-57 avionics power architecture. Since the X-57 electric motors do not have alternators or generators, two 13.8V DC Converters were added to replace the stock Tecnam alternators (Figure 9). Input power to these DC Converters is provide by the high voltage traction battery. The Tecnam stock lead acid battery was replaced with a lithium iron phosphate (LiFePO4) battery. A detailed Avionics Power Analyses were completed for the Mod II configuration and the Mod IV configuration to provide the design requirements for the X-57 Avionics Power System [23, 24]. The Mod II Avionics Power Analysis provided the power requirements for the two 13.8 V DC converters and the lithium iron phosphate battery. Power requirement estimates for each subsystem used in the avionics power analysis were provided by manufacturer specifications, measured in the laboratory or provided by the subsystem design engineer. Typical power requirements and maximum power requirements were provided for each subsystem. The avionics power requirements for the Mod III configuration are the same as the Mod II configuration. In the Mod II /III configuration, vehicle loads were limited to 47% of available power, and to 70% of available power in Mod IV.

The Avionics Power Systems consists of seven 13.8 V buses, two 28 V Buses and two 23 V buses as shown in Figure 5 and each bus is described below. The integration of these buses into the crew workflow to manage the cockpit systems is available in [7].

- Essential Bus, 13.8 V Power for the essential bus is provided by the Lithium Iron Phosphate (LiFePO4) battery. This battery is called the essential battery. The essential bus provides power to enable the two 13.8V DC Converters and essential bus avionics subsystems. If both 13.8V DC Converters were to fail in flight, the essential battery will continue to provide power to essential subsystems and allow the pilot to safely land the aircraft.
- DC Converter Bus A and DC Converter Bus B, 13.8 V These buses are the primary source of avionics power to the aircraft. They provide 13.8 V to the aircraft's avionic systems via the two 13.8V DC Converters. These buses also charge the essential battery in flight. The outputs of these two DC Converters are electrically connected when the Cross Bus relays are closed during startup. Closing the Cross Bus relays allow these DC Converters to share the avionics system load. If one of the DC Converters fail, the other DC Converter can carry the load of the avionics system. The "Mod II Summary" worksheet provides the total estimated power required for the Mod II avionics system. Since the avionics system only uses 47% of the power available from the two DC converters, one converter can provide power to the avionics system if one of the converters failed in flight.
- Avionics Bus A, 13.8 V This bus provides 13.8 V from DC Converter A to non-essential
 avionics subsystems. These subsystems can be turned off if "power shedding" is required in
 flight without affecting the pilot's ability to safely land the aircraft.
- Avionics Bus B, 13.8 V This bus provides 13.8 V from DC Converter B to the input of the
 instrumentation 13.8 V to 28V DC Converter. The instrumentation system requires 28 V. The
 instrumentation system can be turned off if "power shedding" is required in flight without
 affecting the pilot's ability to safely land the aircraft.
- 28 V Bus A and 28 V Bus B The Essential Bus provides input power to two 13.8 V to 28V DC Converters located in BCM A and BCM B. As shown in Figure 19, these DC Converters supply 28 V to enable the high voltage contactors in both the BCM and the Contactor Pallets

which route power to the traction buses. These DC converters also provide power to traction system sensors and displays.

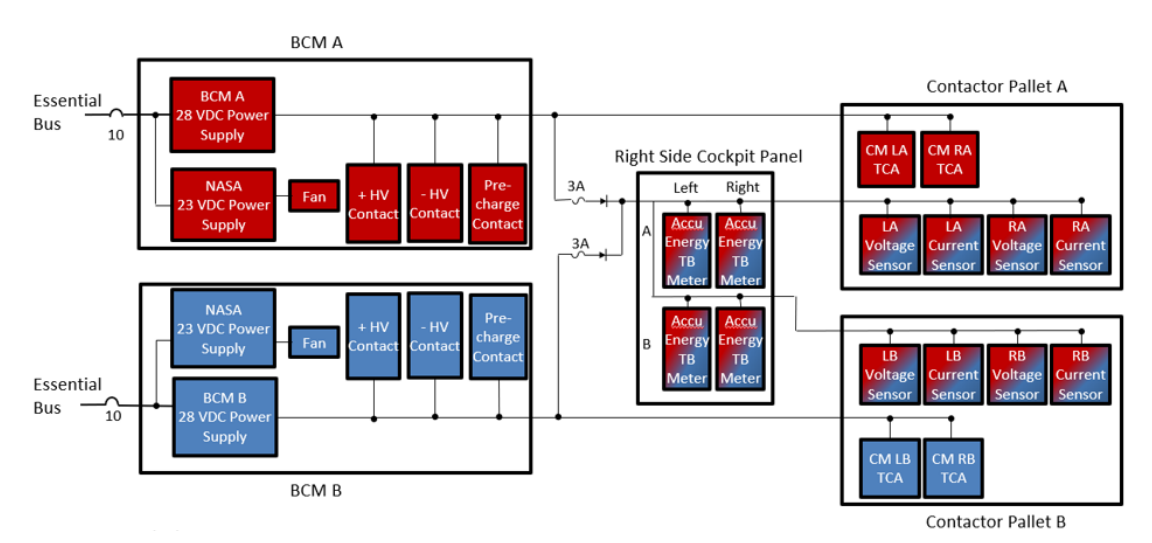


Figure 19 - 28 V Power Distribution

Wing Avionics Bus A and Wing Avionics Bus B, 13.8 V – These buses provides 13.8 V from
the Essential Bus to the input of the of a 13.8 V to 23V DC Converter on each bus. This DC
Converter provides 23 V to avionics subsystems located in the left- and right-wing nacelles.
Each cruise nacelle had a dedicated breaker, and the high lift in Mod IV and A-side and B-side
breaker each powering six nacelles as shown in Figure 20.

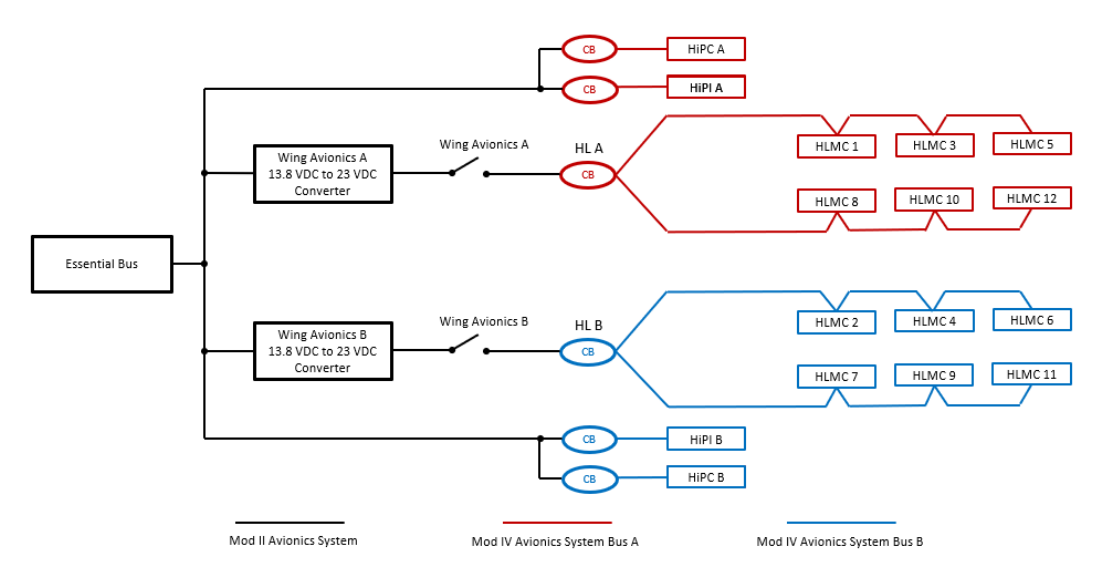


Figure 20 - High Lift System Power Distribution

6 Concluding Remarks

The as-built design of the X-57 Traction, Command, and Avionics subsystems for the Mod II and III vehicle configuration and the final design and partially built components of the Mod IV configuration were reviewed here and effectivity of key design features was considered. The design features discussed included component development insights and system architecture evaluation. Component development features considered included battery storage modules and control modules, cruise and high-lift motors and controller/inverters (both the logical control parts and the traction inverter parts).

The architectures of these subsystems were kept as simple as possible so that any defects that would arise in the experimental components that would comprise these systems would be easy to assess and mitigate. For example, the traction architecture with A-side/B-side and Left/Right redundancy and no safety critical interfaces served the design intent and effectively limited the complexity of failure modes (in number or in effect) which made the hazard analysis simpler. This kept development challenges for these subsystems limited to the components and not the architecture. Electric propulsion powertrains offer great flexibility and opportunity, and a more complex battery or power distribution system would provide more flexibility but also require more development and testing.

Review of these subsystems identified lessons which were described here and in the referenced documents. Lesson topics included, but were not limited to:

- Design and redundancy for electrified propulsion, command, and avionics power systems
- Designing defensively to limit failure modes and effects and contain hazard impacts, both in the direct case to prevent loss of life or equipment damage and in the indirect case to prevent project delays related to failure of prototype hardware late in the development cycle
- Operations considerations on experimental vehicle systems development and on the support equipment that would be required for operating modes needed at various development phases
- Some implementation challenges resulted from architectural choices such direct distribution of battery power to inverters without a regulated voltage converter (mutually constrains motor winding design and battery layout)
- Qualification and acceptance testing to an expected environment was very productive at identifying limits to the hardware design and directing toward improvement

Contact Author Email Address

sean.clarke@nasa.gov

Copyright Statement and Acknowledgements

This material is a work of the U.S. Government and is not subject to copyright protection in the United States. No third-party material is included in this paper.

This work was funded by the NASA Aeronautics Research Mission Directorate. Initial funding came from the Convergent Aeronautics Solutions Project within the Transformational Aeronautics Concepts Program, and funding for later efforts was provided by the Flight Demonstrations and Capabilities Project within the Integrated Aviation Systems Program.

References

- [1] Clarke S, Redifer M, Papathakis K, Samuel A and Foster T. X-57 Power and Command System Design. 2017 IEEE Transportation Electrification Conference and Expo (ITEC), Chicago, IL, USA, pp. 393-400, 2017. Available from NASA at https://ntrs.nasa.gov/citations/20170005797.
- [2] Borer N, Patterson M, Viken J, Moore M, Clarke S et al. Design and Performance of the NASA SCEPTOR Distributed Electric Propulsion Flight Demonstrator. *16th AIAA Aviation Technology, Integration, and Operations Conference*, Washington, DC, USA, 2016. Available from NASA at https://ntrs.nasa.gov/citations/20160010157.
- [3] Deere K, Viken J, Viken S, Carter M, Wiese M et al. Computational Analysis of a Wing Designed for the X-57 Distributed Electric Propulsion Aircraft. *35th AIAA Applied Aerodynamics Conference*, Denver, CO, USA, 2017. Available from NASA at https://ntrs.nasa.gov/citations/20170005883.
- [4] Viken J and Li W X-57 Structural Analysis, Wing Design, & Testing (Statics). Online, 2024. https://ntrs.nasa.gov/citations/20240003425.

- [5] Miller E, Li W, Jordan A and Lung SF. X-57 Wing Structural Load Testing. *AIAA Aviation 2020 Forum*, 2020. Available from NASA at https://ntrs.nasa.gov/citations/20205000798.
- [6] Borer N, Wallace R, Reynolds J, Cox D, Sales C et al. Distributed Thrust Takeoff for the NASA X-57 Mod IV Flight Demonstrator. *34th Congress of the International Council of the Aeronautical Sciences*, Florence, Italy, 2024. Available from NASA at https://ntrs.nasa.gov/.
- [7] Reynolds J, Wallace R, Williams T, Curry A, Harris K et al. Power System Human Machine Interfacesfor the X-57 Mod II Aircraft. AIAA Aviation Forum and ASCEND 2024, Las Vegas, NV, USA, 2024. Available from NASA at https://ntrs.nasa.gov/citations/20240006533.
- [8] Darcy E. Passively Thermal Runaway Propagation Resistant Battery Module that Achieves > 190 Wh/kg. Online, 2016. https://ntrs.nasa.gov/citations/20160003490.
- [9] Darcy E, Darst J, Walker W, Finegan D and Shearing P. Driving Design Factors for Safe, High Power Batteries for Space Applications. Online, 2018. https://ntrs.nasa.gov/citations/20180004170.
- [10] Hernandez Lugo D, Clarke S, Miller T, Redifer M and Foster T. X-57 Maxwell Battery from Cell Level to System Level Design and Testing. Online, 2018. https://ntrs.nasa.gov/citations/20180005737.
- [11] Harris K, Clarke S and Borer N. X-57 Cruise Motor and High-Lift Motor Mission Profile Power Analysis. Online, 2021. https://ntrs.nasa.gov/citations/20230015689.
- [12] Reynolds J, Baumann E, Sales C and Williams T. Flight-Test Approach for X-57 Mod II Configuration. *AIAA Aviation Forum and ASCEND 2024*, Las Vegas, NV, USA, 2024. Available from NASA at https://ntrs.nasa.gov/citations/20240007413.
- [13] Dubois A, van der Geest M, Bevirt J, Clarke S, Christie R et al. Design of an Electric Propulsion System for SCEPTOR's Outboard Nacelle. 16th AIAA Aviation Technology, Integration, and Operations Conference, Washington, DC, USA, 2016. Available from NASA at https://ntrs.nasa.gov/citations/20160007774.
- [14] McLaughlin K, Vidyasagar R, Lucht J, Waddell A, Rudy J et al. X-57 Flight Systems Integration Path. AIAA Aviation Forum and ASCEND 2024, Las Vegas, NV, USA, 2024. Available from NASA at https://ntrs.nasa.gov/citations/20240005892.
- [15] Terry J, Clarke S, Redifer M, Shemenski M, Wilson C et al. NASA X-57 Cruise Motor Controller Airworthiness Test Approach. Online, 2020. https://ntrs.nasa.gov/citations/20205002485.
- [16] Clarke S and Terry J. X-57 Cruise Motor and Inverter Failure Modes. Online, 2024. https://ntrs.nasa.gov/citations/20240003366.
- [17] Kowalewski S, Blystone J, Maroli J, Granger M, Avanesian D et al. NASA's X-57 High Lift Motor Controller: Detailed Design, Test Results, and Outcomes. *AIAA Aviation Forum and ASCEND 2024*, Las Vegas, NV, USA, 2024. Available from NASA at https://ntrs.nasa.gov/citations/20240006334.
- [18] Green C, Conn B and Shemenski M. Test Campaign of X-57 Maxwell's 80kW Electric Propulsion System. *AIAA Aviation 2023 Forum*, San Diego, CA, USA, 2023.
- [19] Bhamidipati K. X-57 Structural Dynamics (Analysis & Testing). Online, 2024. https://ntrs.nasa.gov/citations/20240003367.
- [20] Samuel A and Lin Y. Airvolt Aircraft Electric Propulsion Test Stand. 51st AIAA/SAE/ASEE Joint Propulsion Conference, Orlando, FL, USA, 2015. Available from NASA at https://ntrs.nasa.gov/citations/20160001339.
- [21] Curry A, Clarke S and Samuel A. X-57 Cockpit Display System Development and Features. 2023 AIAA Aviation Forum and Exposition, San Diego, CA, USA, 2023. Available from NASA at https://ntrs.nasa.gov/citations/20230005312.
- [22] Borer N and Patterson M. X-57 High-Lift Propeller Control Schedule Development. AIAA Aviation 2020 Forum. Available from NASA at https://ntrs.nasa.gov/citations/20205010303.
- [23] Harris K. X-57 Mod II Avionics Power Analysis. Online, 2023. https://ntrs.nasa.gov/citations/20230015691.
- [24] Harris K. X-57 Mod IV Avionics Power Analysis. Online, 2023. https://ntrs.nasa.gov/citations/20230015625.